

### EVL6591-90WADP: 90 W AC-DC asymmetrical half-bridge adapter using L6591 and L6563

#### Introduction

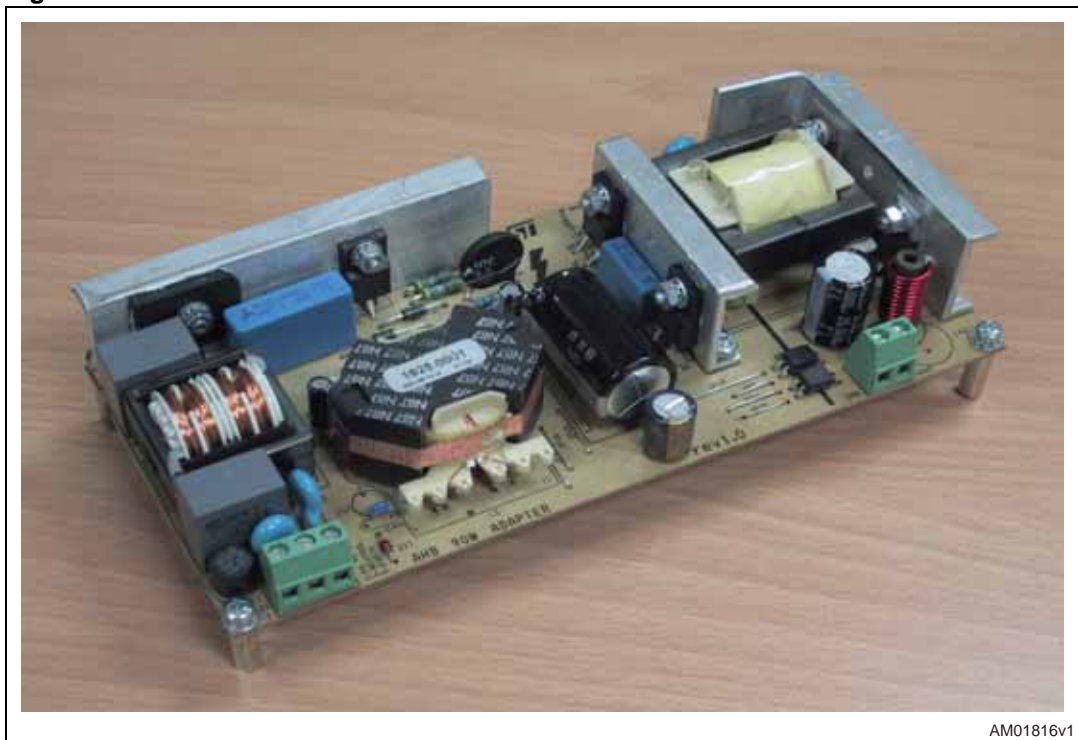
This document describes the characteristics and performance of a 90 W wide range input AC-DC adapter based on asymmetrical half-bridge topology (AHB).

The converter comprises a two-stage approach: a PFC front-end stage using the L6563 TM PFC controller and a DC-DC stage that implements the asymmetrical half-bridge (AHB) topology driven by the L6591, the new PWM controller dedicated to this architecture.

Thanks to the AHB topology, the system offers good electrical performance (EPA 2.0 compliant) with a low-voltage and high-current output (12 V - 7.5 A).

The order code for this demonstration board is EVL6591-90WADP.

**Figure 1. EVL6591-90WADP demonstration board**



AM01816v1

# Contents

<b>1</b>	<b>Main characteristics and circuit description</b>	<b>4</b>
<b>2</b>	<b>Operating waveforms</b>	<b>7</b>
2.1	Asymmetrical half-bridge (AHB) typical waveforms	7
2.2	Low-load operation	10
2.3	Short-circuit protection	12
2.4	Overvoltage protection	13
2.5	Startup sequence	15
<b>3</b>	<b>Electrical performance</b>	<b>17</b>
3.1	Efficiency measurement and no-load consumption	17
3.2	Harmonic content measurement	20
<b>4</b>	<b>Thermal measurements</b>	<b>22</b>
<b>5</b>	<b>Conducted noise measurements (pre-compliance test)</b>	<b>24</b>
<b>6</b>	<b>Bill of material</b>	<b>25</b>
<b>7</b>	<b>PFC coil specifications</b>	<b>29</b>
7.1	Electrical characteristics	29
7.2	Mechanical aspect and pin numbering	30
<b>8</b>	<b>AHB transformer specifications</b>	<b>31</b>
8.1	Electrical characteristics	31
8.2	Mechanical aspect and pin numbering	32
<b>9</b>	<b>PCB layout</b>	<b>33</b>
<b>10</b>	<b>Revision history</b>	<b>34</b>

## List of figures

Figure 1.	EVL6591-90WADP demonstration board . . . . .	1
Figure 2.	EVL6591-90WADP schematic . . . . .	6
Figure 3.	AHB primary side key waveforms at full load . . . . .	7
Figure 4.	Detailed AHB zero-voltage switching at full load . . . . .	8
Figure 5.	Detailed AHB zero-voltage switching at half load . . . . .	9
Figure 6.	AHB secondary side key waveforms at full load . . . . .	9
Figure 7.	Burst mode at no load . . . . .	10
Figure 8.	Detailed burst mode at no load . . . . .	11
Figure 9.	Load transitions . . . . .	11
Figure 10.	Detailed short-circuit behavior . . . . .	12
Figure 11.	HICCUP mode . . . . .	13
Figure 12.	Detailed OVP intervention . . . . .	14
Figure 13.	OVP intervention: system is latched . . . . .	14
Figure 14.	Complete startup sequence at 115Vac and full load . . . . .	15
Figure 15.	Detailed startup sequence at 115Vac and full load . . . . .	16
Figure 16.	Efficiency vs. O/P power . . . . .	18
Figure 17.	No-load consumption . . . . .	19
Figure 18.	EN61000-3-2 measurements at full load . . . . .	20
Figure 19.	JEIDA-MITI measurements at full load . . . . .	20
Figure 20.	EN61000-3-2 measurements at 75 W input . . . . .	20
Figure 21.	JEIDA-MITI measurements at 75 W input . . . . .	20
Figure 22.	PF vs. input voltage . . . . .	21
Figure 23.	THD vs. input voltage . . . . .	21
Figure 24.	Thermal map at 115Vac - full load . . . . .	22
Figure 25.	Thermal map at 230Vac - full load . . . . .	22
Figure 26.	CE peak measure at 115Vac and full load . . . . .	24
Figure 27.	CE peak measure at 230Vac and full load . . . . .	24
Figure 28.	Electrical diagram . . . . .	29
Figure 29.	Bottom view . . . . .	30
Figure 30.	Electrical diagram . . . . .	31
Figure 31.	Windings position . . . . .	32
Figure 32.	Top view . . . . .	32
Figure 33.	Topside silk screen . . . . .	33
Figure 34.	Bottomside silk screen . . . . .	33
Figure 35.	Copper traces (bottomside) . . . . .	33

# 1 Main characteristics and circuit description

The main characteristics of the SMPS adapter are as follows:

- Input mains range
  - $V_{in}$ : 88 ~ 264 Vrms
  - $f$ : 45 ~ 66 Hz
- Output: 12Vdc  $\pm$  2% - 7.5 A
- No-load: Pin below 0.35 W
- Protections
  - Short-circuit
  - Overload
  - Output overvoltage
  - Brownout
- PCB type and size
  - CEM-1
  - Single-side 70  $\mu$ m
  - 174 x 78 mm
- Safety: according to EN60065
- EMI: according to EN50022 - class B

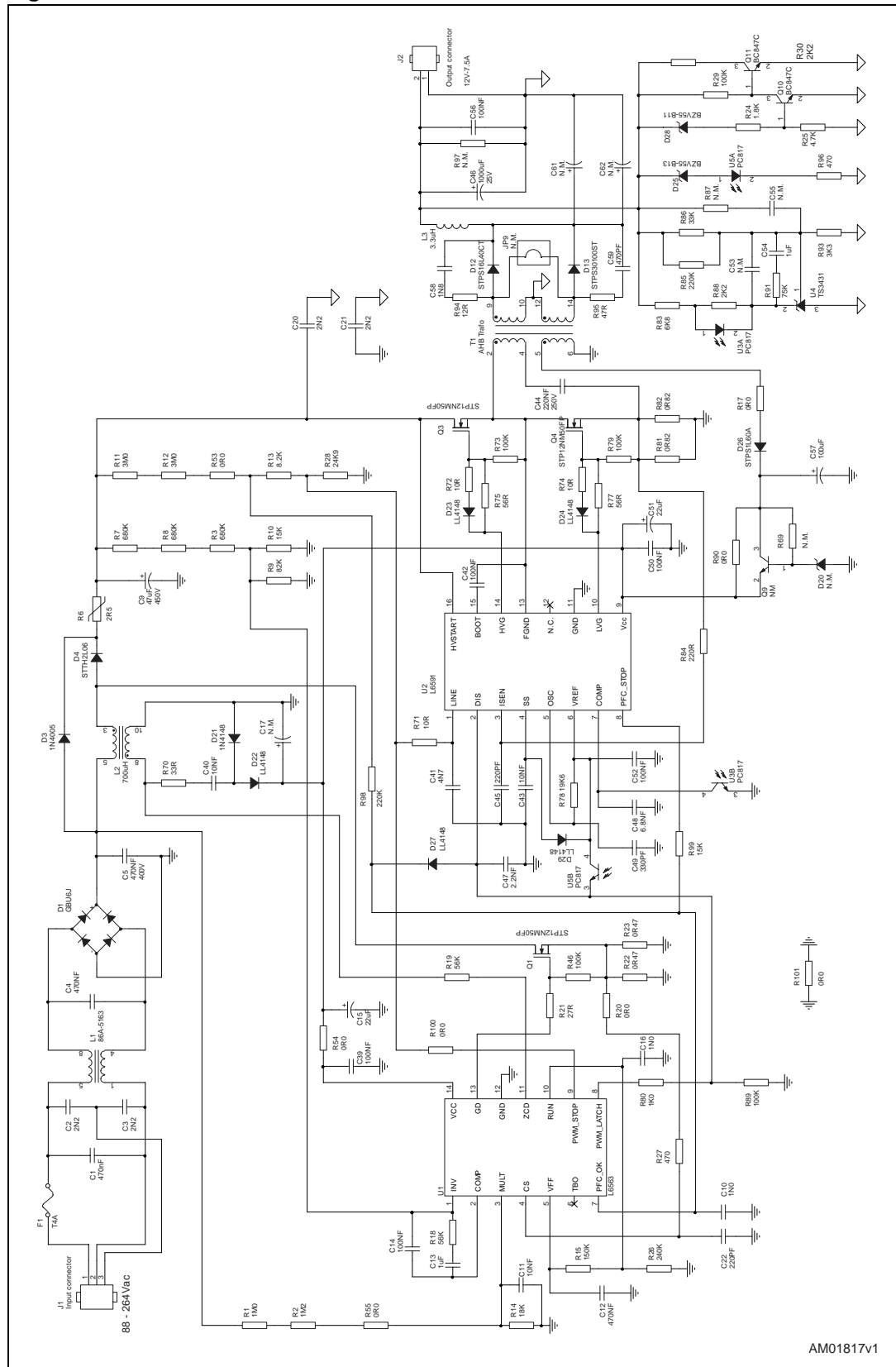
The adapter implements a two-stage solution. The front-end PFC uses a boost topology working in transition mode (TM). The IC used is the L6563, advanced TM PFC controller, which integrates all the functions and protection needed to control the stage and an interface with the downstream DC-DC converter.

The power stage of the PFC comprises inductor L2, MOSFET Q1, diode D4 and capacitor C9. The PFC circuit is quite standard and already well described in previous ST application notes. Therefore this note will focus on the AHB stage and its controller, the L6591. This DC-DC converter comprises a half-bridge (MOSFET Q3 and Q4) connected to the output voltage of the PFC stage that drives the series connection of a DC blocking capacitor (C44) and the primary of the transformer (T1). The transformer has two secondary windings with a center tap connection tied to ground. The other ends are connected to the output diodes D12 and D13. The output inductor is between the common cathode of diodes D12 and D13 and the output. The L6591 includes a current mode PWM controller (fixed-frequency solution), gate drivers for both low and high-side MOSFETs with integrated bootstrap diode and all the functions and protections tailored for this topology. The device is housed in an SO-16 narrow package.

This adapter uses the magnetizing current and the output inductor current ripple to obtain the correct primary current direction to achieve zero-voltage switching (ZVS) at turn-on of both MOSFETs. The transformer construction is quite simple as it is a layer type with the primary winding split in two parts (sandwich configuration) and two secondary windings. The primary leakage inductance is about 3% of the magnetizing inductance. The half-bridge is operated at fixed frequency with complementary duty cycles on the two MOSFETs. The high-side FET is on during the D time and the low-side FET is on for the 1-D time. C44 is calculated in order to have a resonance frequency due to  $L_m$  and C44 well below the switching frequency (that, in this application, has been set at about 100 kHz). In this way the voltage on C44 is nearly constant and equal to  $V_{in} \times D$  where  $V_{in}$  is the high-voltage input

bus and  $D$  is the duty cycle. For stability reasons related to the topology, the IC limits the maximum duty cycle at 50%. The current in the primary tank circuit is read by the controller thanks to the sense resistors R81 and R82. The self supply is basically obtained thanks to an auxiliary winding on the AHB transformer. A small charge pump on the auxiliary windings of the PFC inductor helps during the startup phase. A pin dedicated to startup sequencing, a spare latched protection (dedicated here to output overvoltage protection), the soft-start function, the overload protection, an interface with the PFC controller and the integrated high-voltage startup generator complete the features of the L6591. All the functions and protections are detailed in the following sections.

Figure 2. EVL6591-90WADP schematic



AM01817v1

## 2 Operating waveforms

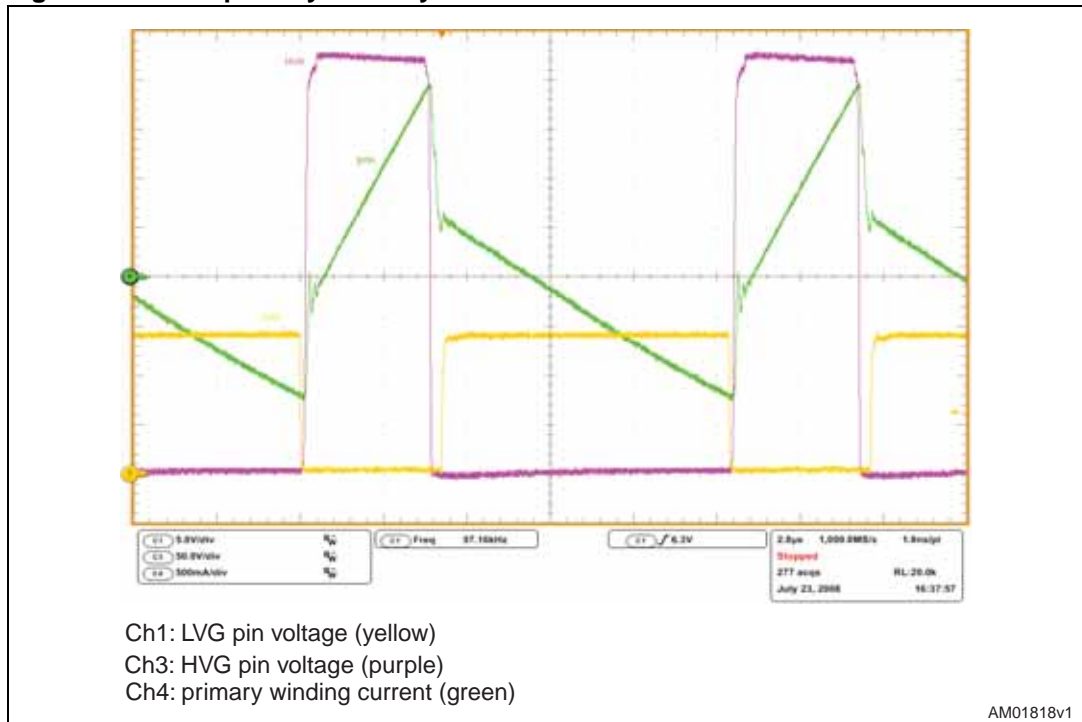
### 2.1 Asymmetrical half-bridge (AHB) typical waveforms

As mentioned before, this application note focuses on the AHB stage. This DC-DC converter has the 400 V PFC bus as input and delivers 12 V at the output.

In [Figure 3](#) the primary side key waveforms with full load applied are shown. [Figure 4](#) shows the detail of the two transitions during one switching cycle. When the LVG signal goes down, the current is negative and so the half-bridge node (that has a certain capacitance value due to the  $C_{oss}$  of the MOSFETs and the stray capacitance of the circuit) is charged up to 400 V. After the deadtime has elapsed the high-side driver is turned on with zero volts across the high-side MOSFET drain-source pins. The driver activation is visible on the HVG signal when there is the small voltage step on the high part of the waveform.

When the high-side driver is turned off, the primary current is positive, so the half-bridge node is discharged down to zero volts and the body diode of Q4 is activated. After the deadtime the LVG turns on in ZVS condition.

**Figure 3. AHB primary side key waveforms at full load**

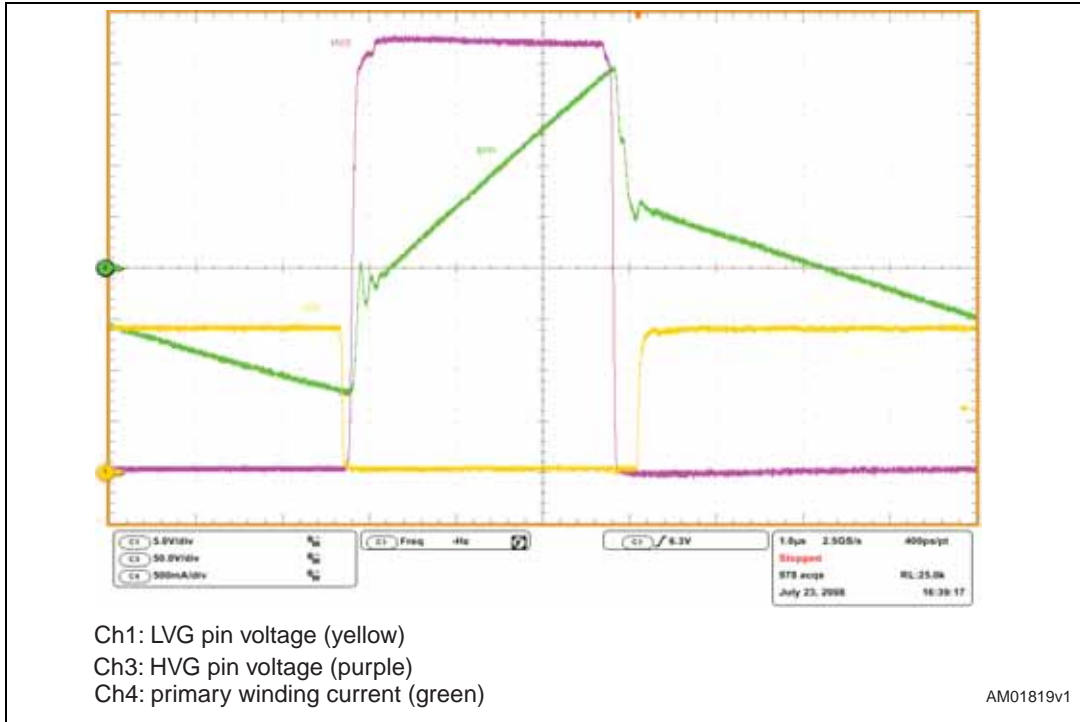


Typically, in the AHB topology, the most critical transition is the one between LVG turn-off and HVG turn-on. In fact it is visible that the current available to move the half-bridge point is less with respect to the other transition. This is due to the magnetizing current that is not symmetrical with an average value of zero amps but has a certain offset due to the asymmetrical driving of the tank circuit.

The fast current variation during transitions is due to the reversal of the current direction in the secondary windings. The effort in this design was to maintain a negative current after

the positive variation at LVG turn-off. This was done by a correct design of the magnetizing current, output inductor current ripple and choice of turns ratio.

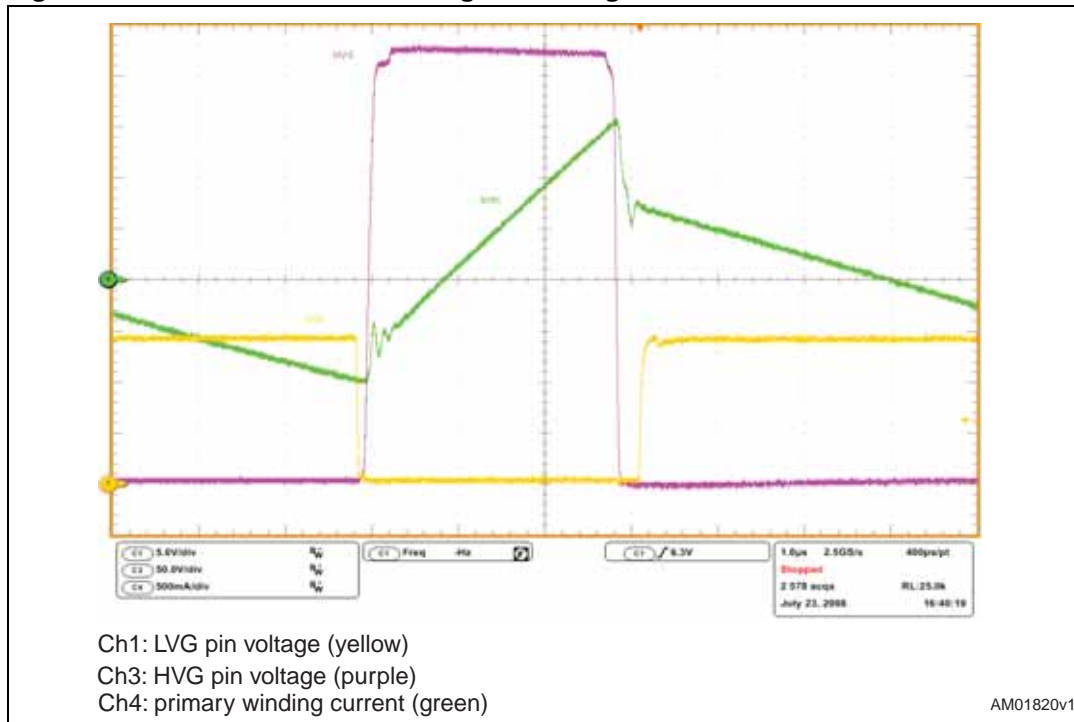
**Figure 4. Detailed AHB zero-voltage switching at full load**



The ZVS condition is harder to meet as the load increases, so full load is the worst condition to have for a correct ZVS operation. In [Figure 5](#) the same waveforms are shown with half load. Since the output current is reduced, the fast primary side current variations are also reduced and so the magnetizing current (that remains basically the same if the load changes) becomes proportionally higher. The result is that there is more current available for moving the half-bridge node.

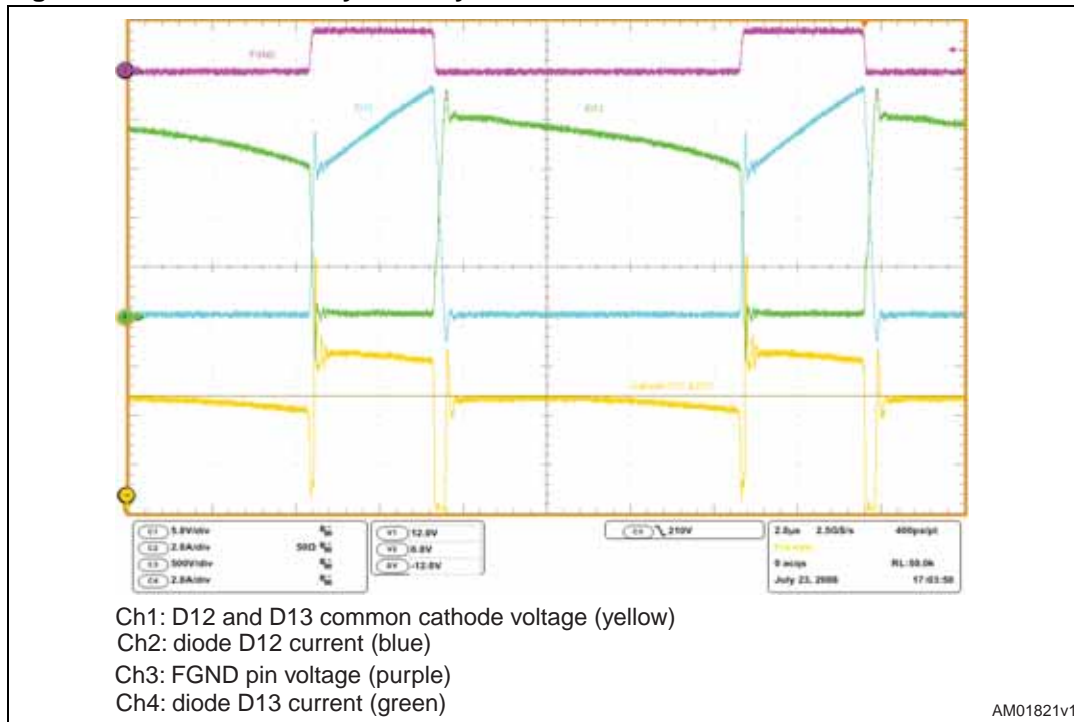


Figure 5. Detailed AHB zero-voltage switching at half load



The key waveforms at the secondary side are shown in [Figure 6](#). It is interesting to note that, while the current is swapped between the two diodes, the voltage at their cathode is nearly zero.

Figure 6. AHB secondary side key waveforms at full load



Another peculiarity of this topology is that, since it is asymmetrical, the diode D13 has to carry higher average and RMS current and sustain higher reverse voltage with respect to diode D12. This implies that D13 dissipates a lot more than D12 and makes sense, in order to improve efficiency and save money, to have a synchronous rectification only on D13.

## 2.2 Low-load operation

At light loads (and no-load) conditions the system enters a controlled burst mode operation, allowing input power reduction. The burst mode is activated according to the COMP pin level.

In [Figure 7](#) and [Figure 8](#) the burst mode operation with no load is shown. Under a certain load also the PFC stage works in burst mode operation (specifically the PFC enters in burst mode for a load value higher than the one for the AHB). Using the PFC\_STOP pin of the L6591 and the PFC\_OK pin of the L6563, a simple interface is built in order to keep the burst modes of the two ICs synchronized. This operation allows fast response to a heavy load transition since the PFC is already on when the power is needed. This avoids output voltage dips. The load transition from 0 to 100% and vice versa can be seen in [Figure 9](#).

**Figure 7. Burst mode at no load**

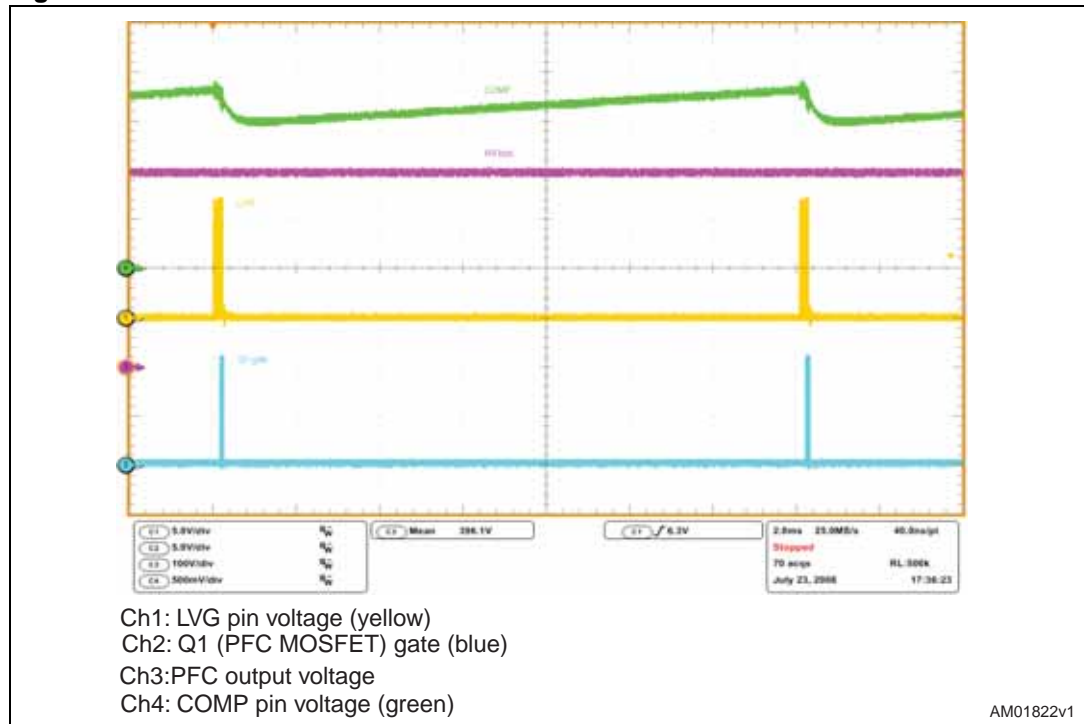


Figure 8. Detailed burst mode at no load

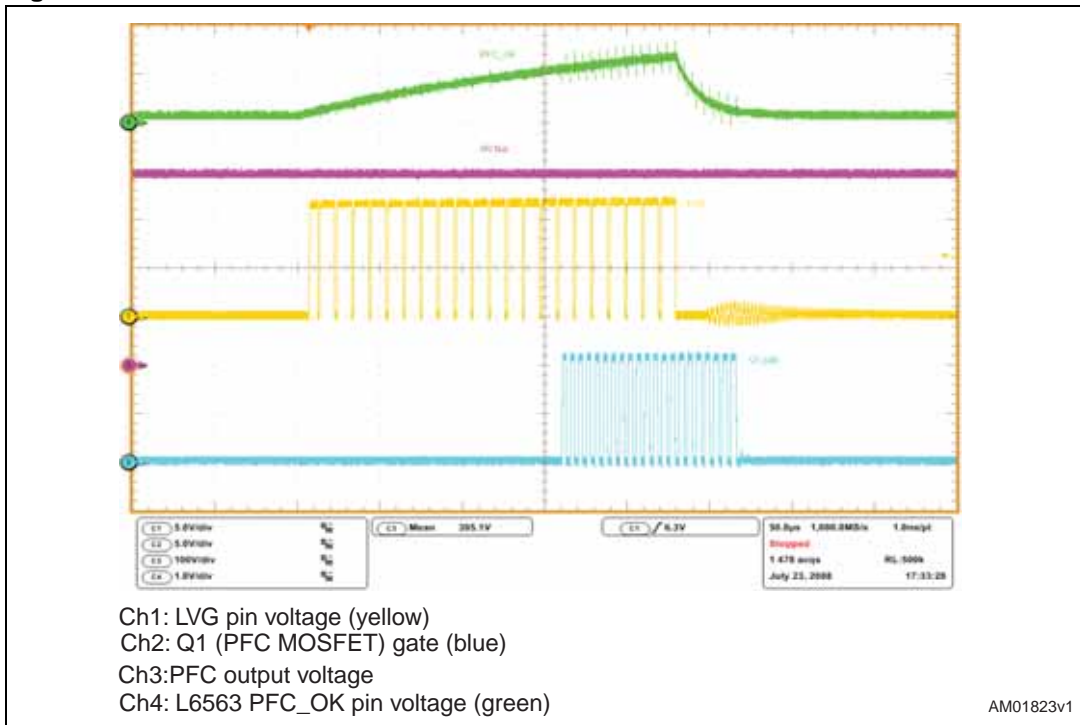
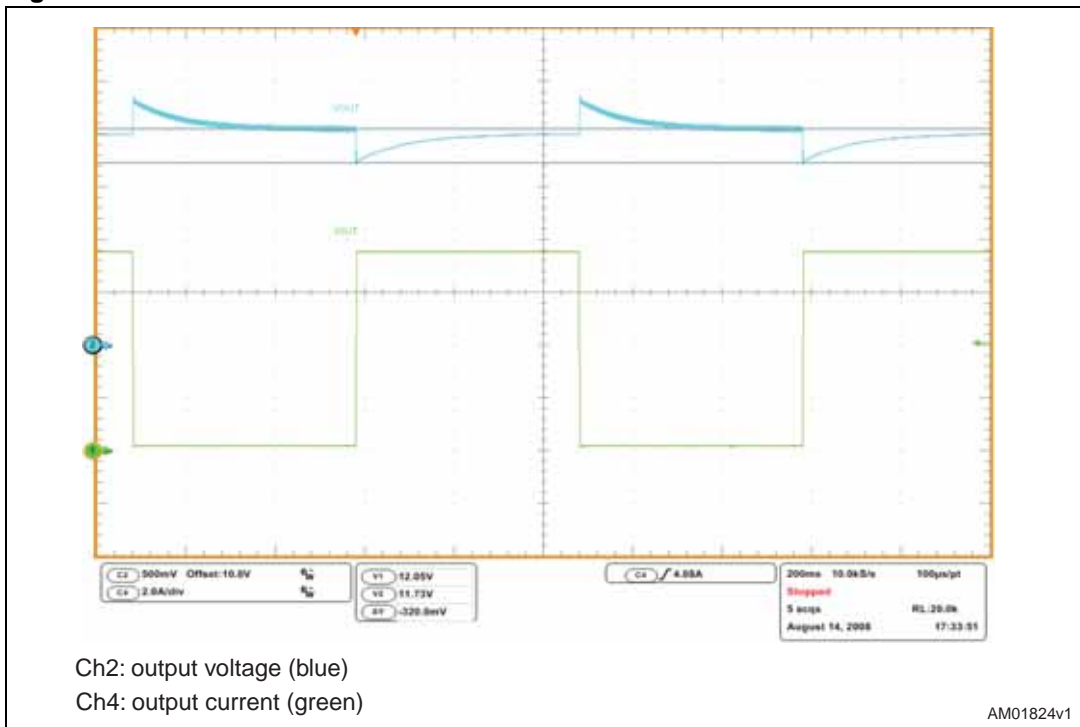


Figure 9. Load transitions



## 2.3 Short-circuit protection

A short-circuit at the output activates the overload protection (OLP). *Figure 10* shows the pins involved in this function. When the short-circuit is applied, the COMP pin saturates high. The IC detects this condition and starts charging the SS capacitor. When the SS voltage reaches 5 V, the system shuts down. Diode D29 allows the SS voltage to be clamped at about 5.4 V and the protection has an auto-restart behavior. If the short circuit is not removed, the IC enters the HICCUP mode (*Figure 11*). When the IC is stopped by the OLP, the high-voltage startup generator is invoked only when  $V_{CC}$  falls to 5 V ( $V_{CC_{restart}}$ ). Thanks to this approach, the period between two restart trials is quite long which reduces the stress on power components.

**Figure 10. Detailed short-circuit behavior**

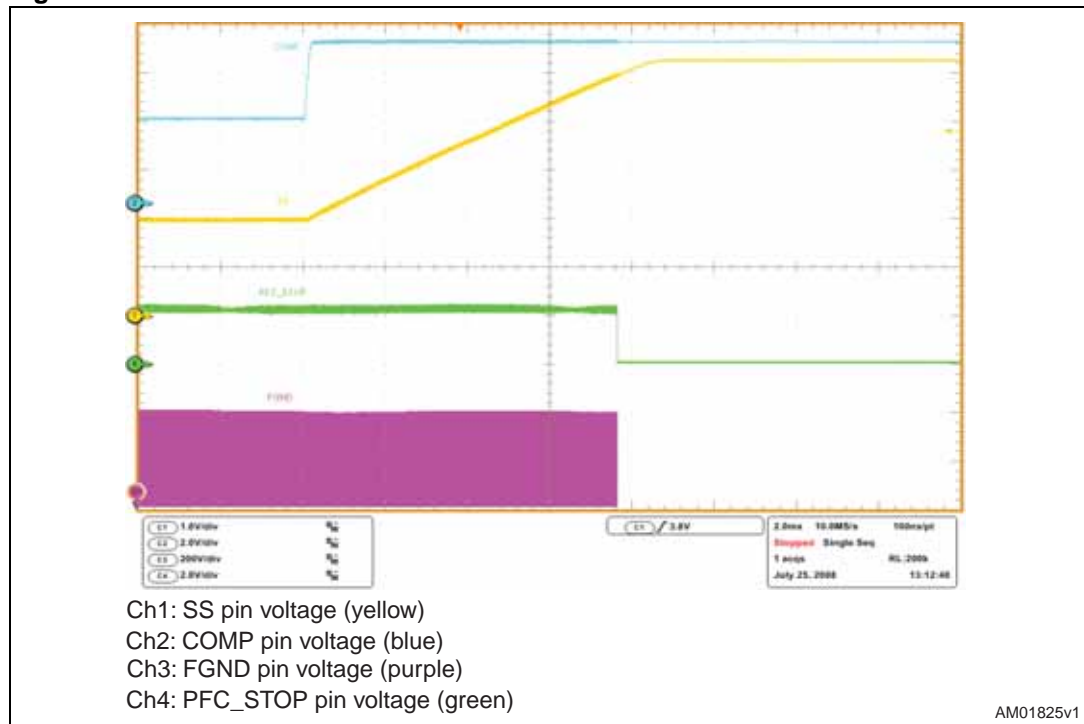
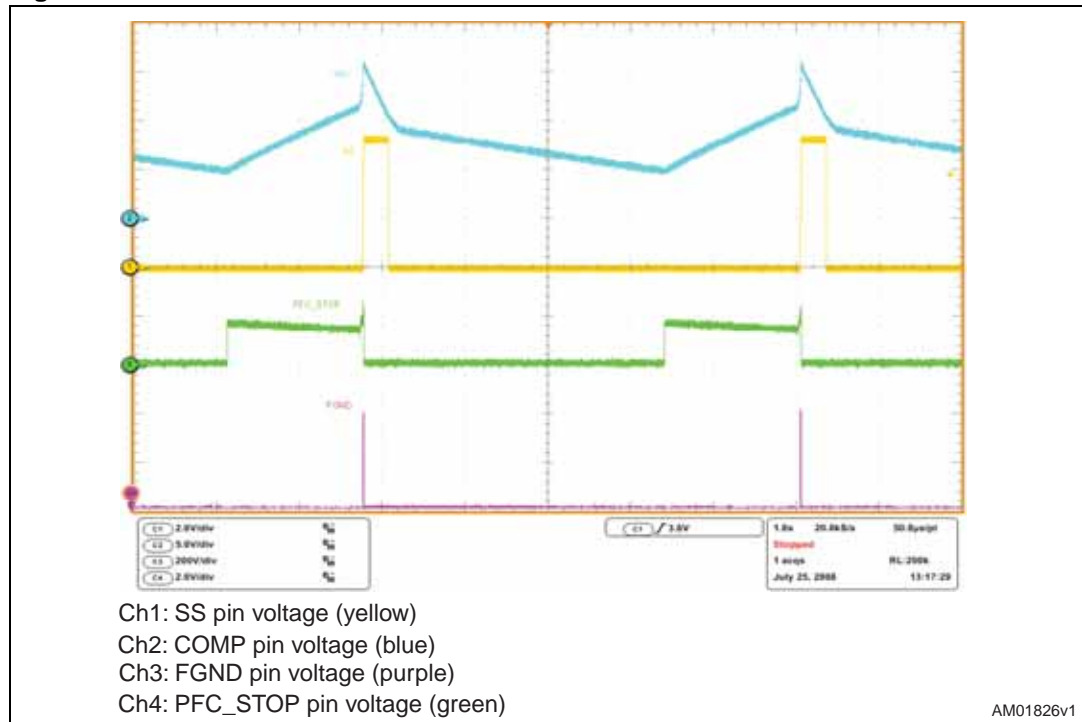


Figure 11. HICCUP mode



## 2.4 Overvoltage protection

Since it is impossible to sense the output voltage from the primary side in all load conditions, the OVP senses such voltage directly on the output. A Zener diode (D25) is used as the threshold to activate the protection. The information is passed to the controller using optocoupler U5 that increases the disable pin voltage over the intervention threshold of 4.5 V. In [Figure 12](#) a loop failure is simulated by shorting R93. The overvoltage protection is invoked and the output voltage reaches a maximum voltage of 14.8 V.

Since this protection uses the disable pin, it is latched. Hence, after PWM is stopped, the HV generator is invoked to keep Vcc voltage between 14 V and 13.5 V. Diode D27 brings the PFC\_OK pin voltage over 2.5 V, so the L6563 is also shut down and its consumption goes almost to the startup level. The PWM\_LATCH goes high which also keeps the disable pin high. The latched operation is shown in [Figure 13](#).

Figure 12. Detailed OVP intervention

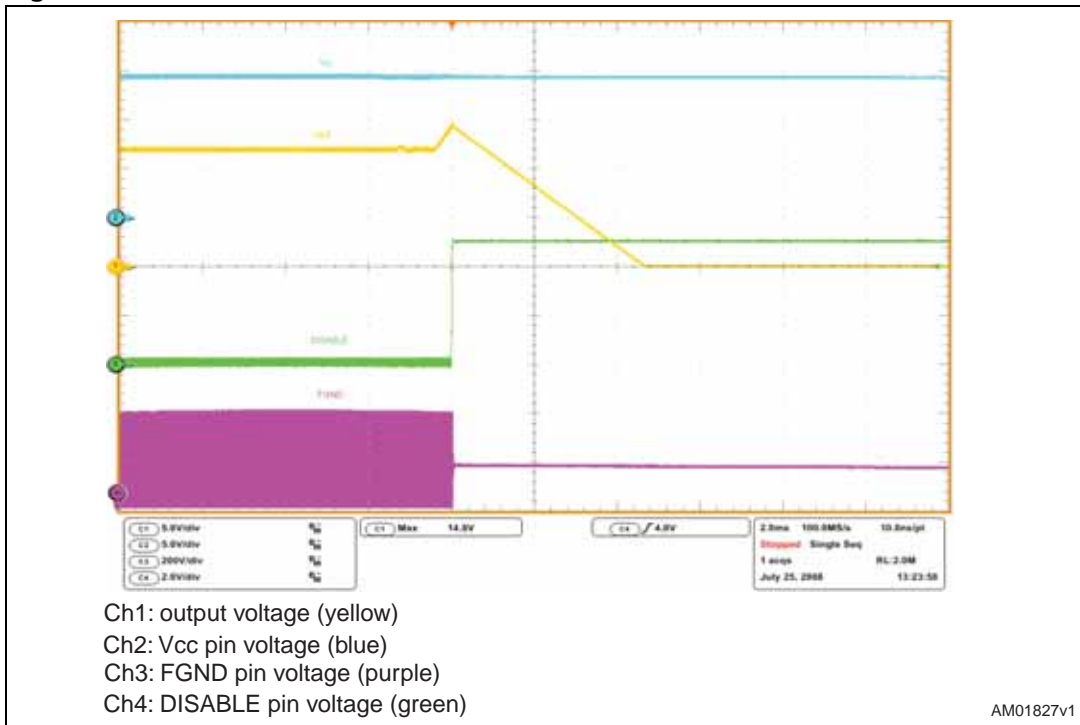
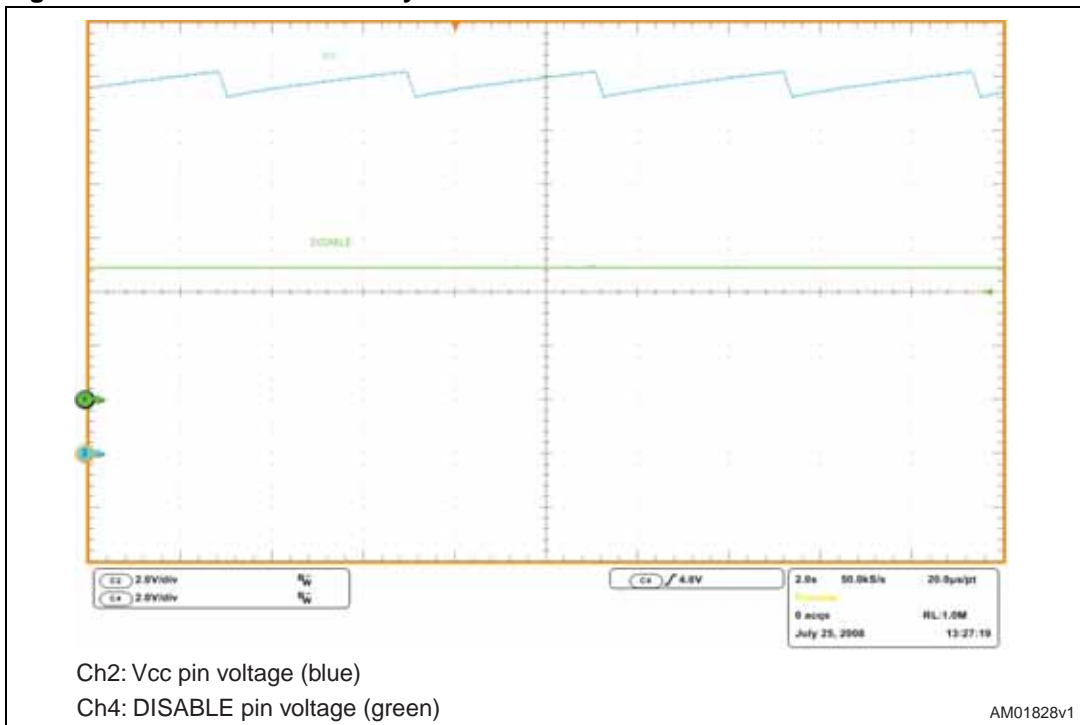


Figure 13. OVP intervention: system is latched



## 2.5 Startup sequence

In this converter the startup sequence is quite particular and merits a detailed explanation.

When the mains is plugged in, the rectified input voltage is present on bulk capacitor C9. Since this value is greater than 80 V, the HV startup generator of the L6591 is turned on and Vcc capacitors are charged with a constant current of about 0.75 mA. This charge time is therefore independent of input voltage level. The L6563 has a turn-on threshold lower than that of L6591, so the PFC controller starts first. The HV startup current is insufficient to power the L6563, so a small charge pump (R70, C40, D21 and D22) is connected to the PFC inductor auxiliary winding. With this circuit, when the L6563 starts, both Vcc voltage and PFC output voltage increase.

Once  $V_{cc} > 14$  V and line pin voltage is greater than 1.25 V, the L6591 also turns on. At this point the charge pump is insufficient to sustain Vcc current of both ICs and so an auxiliary winding on the AHB transformer is used to provide, together with the charge pump, the power requested by the devices. The complete sequence is shown in [Figure 14](#), while the details of the turn-on of both ICs are shown in [Figure 15](#). Both figures show the startup at 115Vac mains input. The startup at 230Vac is very similar, the only difference is that the Vcc voltage during steady state operation is a little higher since the charge pump delivers more current.

**Figure 14. Complete startup sequence at 115Vac and full load**

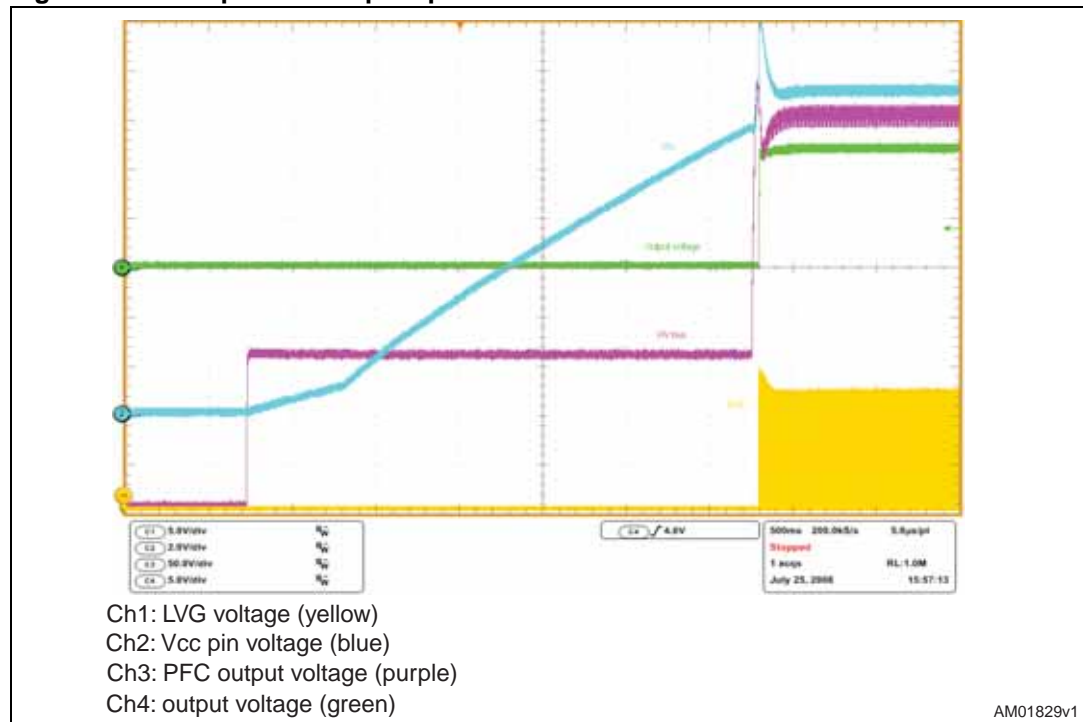
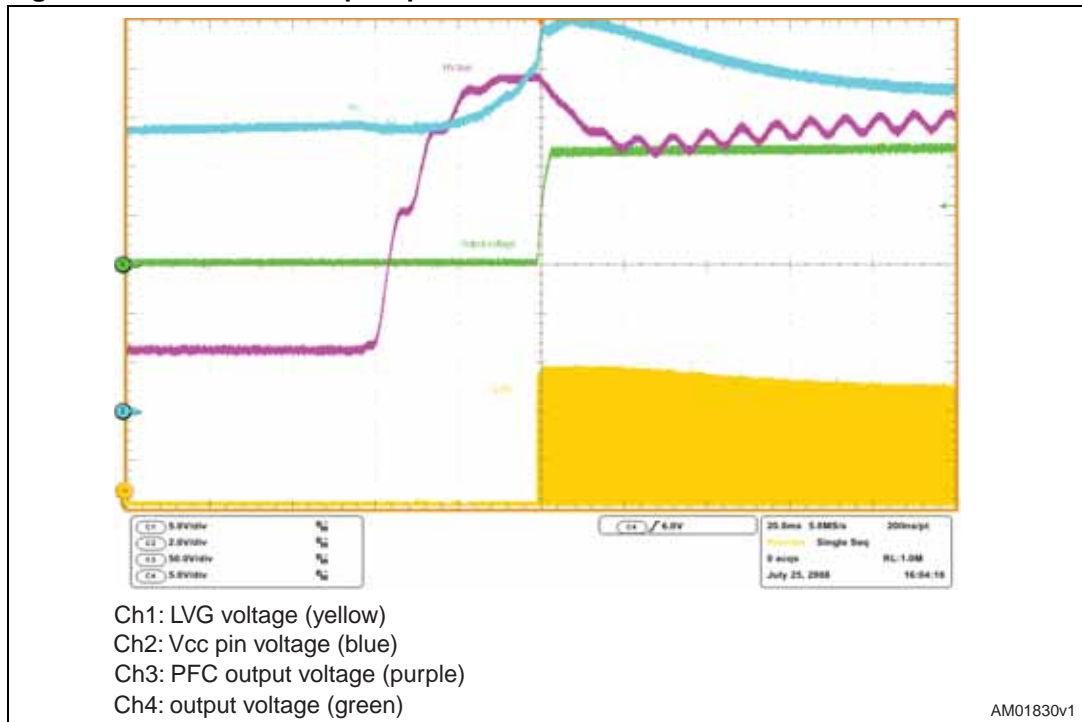


Figure 15. Detailed startup sequence at 115Vac and full load





### 3 Electrical performance

#### 3.1 Efficiency measurement and no-load consumption

*Table 1* and *2* give the efficiency measurements taken at the two nominal voltages.

**Table 1. Efficiency at 115Vrms**

Load [%]	Iout [A]	Vout [V]	Pout [W]	Pin [W]	Eff [%]
5%	0.3746	12.12	4.54	6.80	66.77%
10%	0.7507	12.11	9.09	12.10	75.13%
20%	1.5037	12.10	18.19	21.98	82.78%
25%	1.8787	12.09	22.71	26.83	84.66%
40%	3.0037	12.09	36.31	41.49	87.53%
50%	3.7537	12.08	45.34	51.41	88.20%
60%	4.5037	12.08	54.40	61.44	88.55%
75%	5.6287	12.07	67.94	76.67	88.61%
80%	6.0037	12.07	72.46	81.77	88.62%
100%	7.5037	12.06	90.49	102.48	88.30%

**Table 2. Efficiency at 230Vrms**

Load [%]	Iout [A]	Vout [V]	Pout [W]	Pin [W]	Eff [%]
5%	0.3746	12.12	4.54	6.58	68.97%
10%	0.7507	12.11	9.09	12.41	73.26%
20%	1.5037	12.10	18.19	22.30	81.59%
25%	1.8787	12.09	22.71	27.02	84.06%
40%	3.0037	12.08	36.28	41.37	87.71%
50%	3.7537	12.08	45.34	51.05	88.82%
60%	4.5037	12.07	54.36	60.83	89.36%
75%	5.6287	12.07	67.94	75.60	89.87%
80%	6.0037	12.07	72.46	80.56	89.95%
100%	7.5037	12.06	90.49	100.55	90.00%

The efficiency taken at 25%, 50%, 75% and 100% of rated load allows calculating the average efficiency required by the ENERGY STAR® specification.

**Table 3. Average efficiency for EPA**

Vin [Vrms]	Average efficiency for EPA
115	87.44%
230	88.19%

Table 4 shows the no-load consumption. The adapter has good values (about 300 mW at 230Vac), considering that it is a two-stage system with the PFC stage always on.

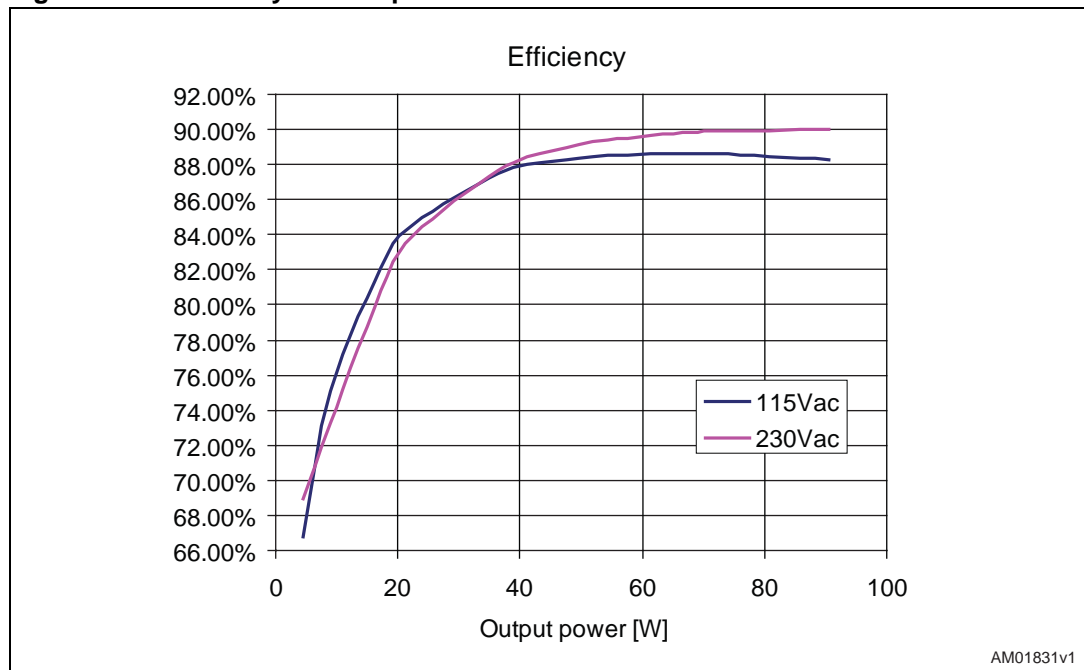
**Table 4. No-load consumption**

Vin [Vac]	90	115	135	180	230	264
Pin [W]	0.215	0.225	0.235	0.255	0.290	0.315

This adapter meets the two conditions required by ENERGY STAR® specification version 2.0 (average efficiency > 87% and no-load input power < 0.5 W) for an external power supply (EPS). Therefore this SMPS is EPA 2.0 compliant.

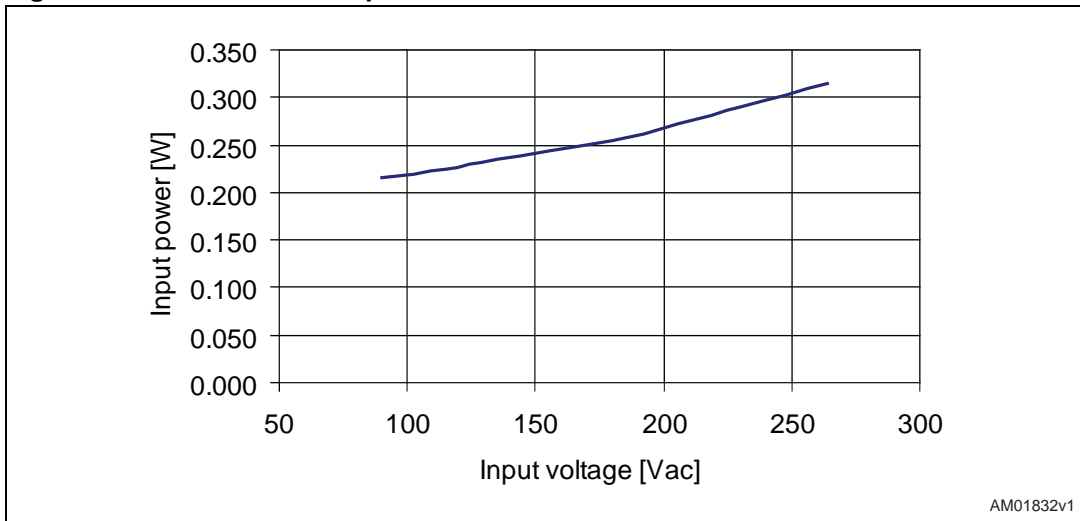
Figure 16 shows the graph of the efficiency vs. output power while Figure 17 shows the graph of the input power vs. input voltage with no load applied.

**Figure 16. Efficiency vs. O/P power**



AM01831v1

Figure 17. No-load consumption



Some measurements with low output loads were also taken, refer to [Table 5](#) and [Table 6](#).

Table 5. Low-load efficiency at 115Vrms

Pout [W]	Iout [mA]	Vout [V]	Pin [W]	Eff [%]
1.50	124.50	12.12	2.696	55.97%
1.00	82.50	12.12	1.883	53.10%
0.50	42.02	12.12	1.076	47.31%
0.25	21.05	12.11	0.654	38.98%

Table 6. Low-load efficiency at 230Vrms

Pout [W]	Iout [mA]	Vout [V]	Pin [W]	Eff [%]
1.50	124.50	12.12	2.598	58.08%
1.00	82.50	12.12	1.802	55.49%
0.50	42.02	12.12	1.087	46.83%
0.25	21.05	12.11	0.704	36.21%

### 3.2 Harmonic content measurement

The front-end PFC stage provides the reduction of the mains harmonic, allowing meeting European EN61000-3-2 and Japanese JEIDA-MITI standards for class D equipment.

Figure 18 and 19 show the harmonic contents of the mains current at full load.

A measure has been done also with 75 W input power which is the lower limit for using harmonic reduction techniques.

Figure 18. EN61000-3-2 measurements at full load

Figure 19. JEIDA-MITI measurements at full load

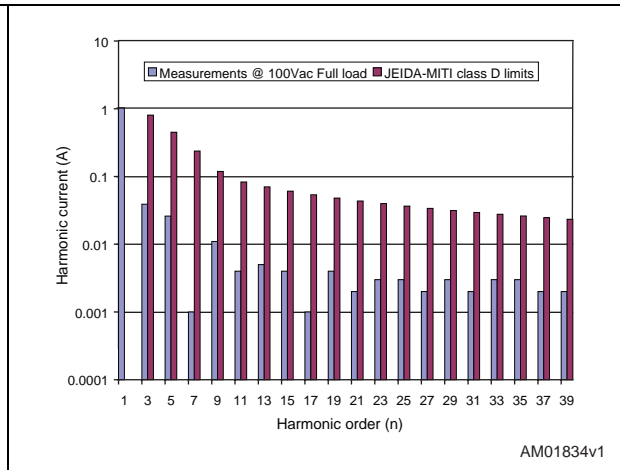
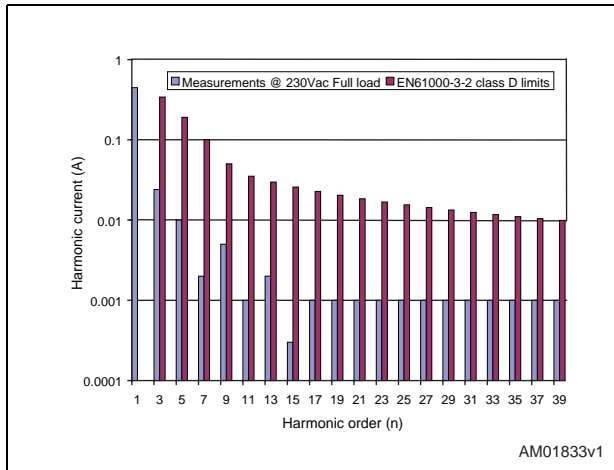
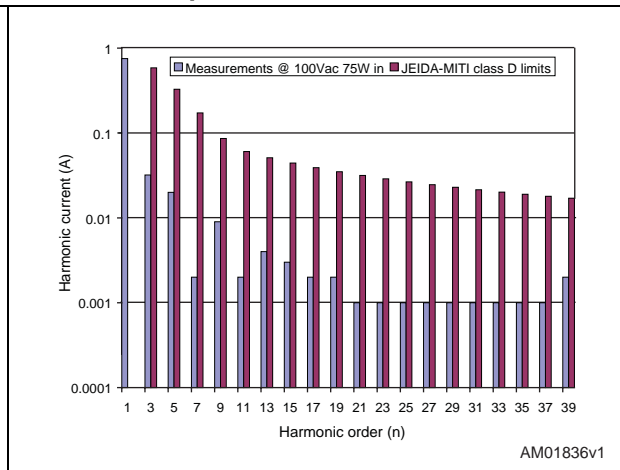
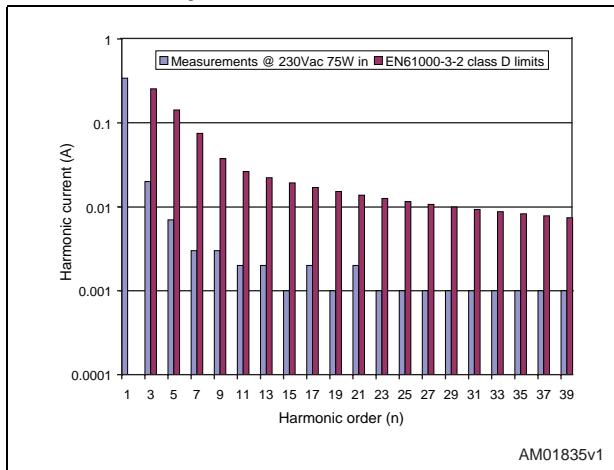


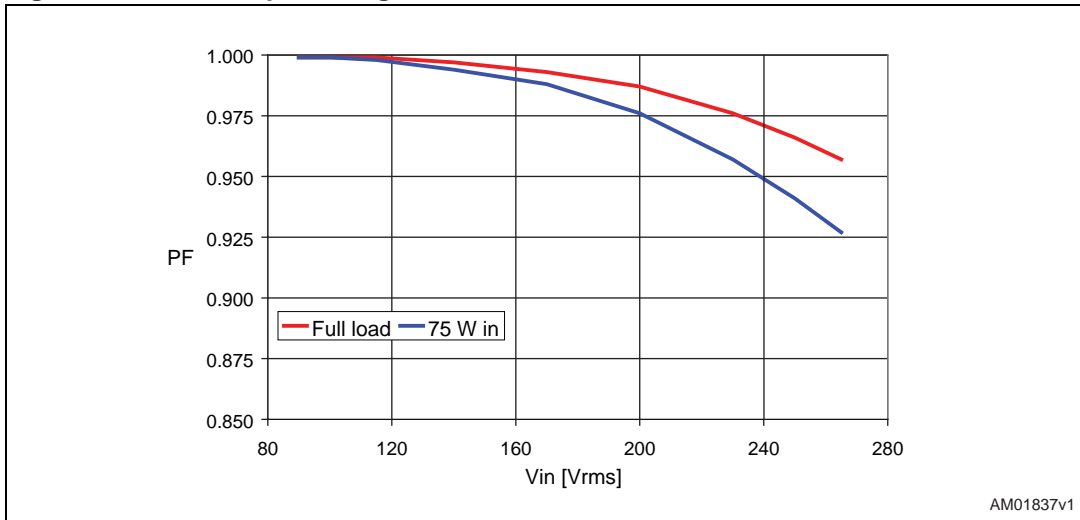
Figure 20. EN61000-3-2 measurements at 75 W input

Figure 21. JEIDA-MITI measurements at 75 W input

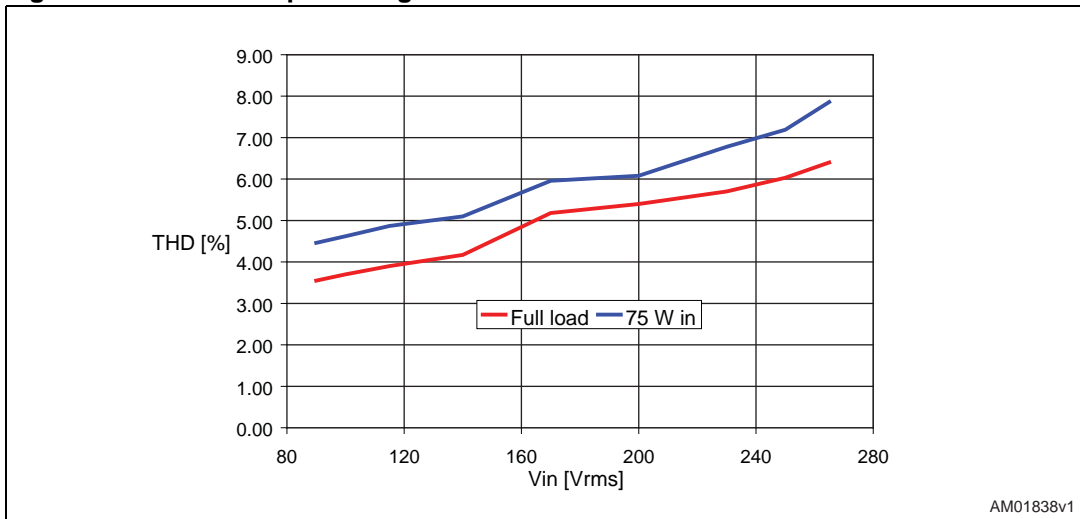


To evaluate the performance of the PFC stage also, the PF and THD vs. input voltage graphs are shown in [Figure 22](#) and [23](#) at full load and 75 W input power.

**Figure 22. PF vs. input voltage**



**Figure 23. THD vs. input voltage**



## 4 Thermal measurements

A thermal analysis of the board was performed using an IR camera, refer to [Figure 24](#) and [25](#).

**Figure 24. Thermal map at 115Vac - full load**

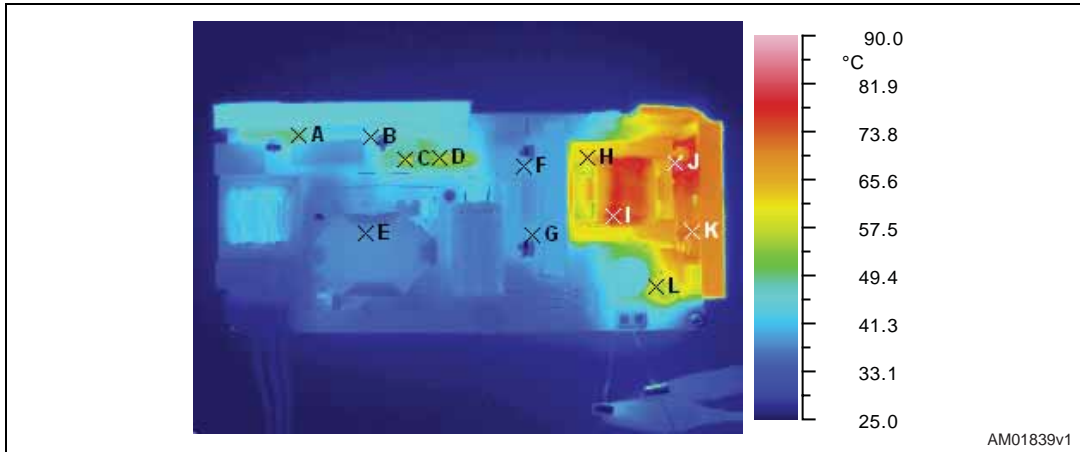


**Figure 25. Thermal map at 230Vac - full load**

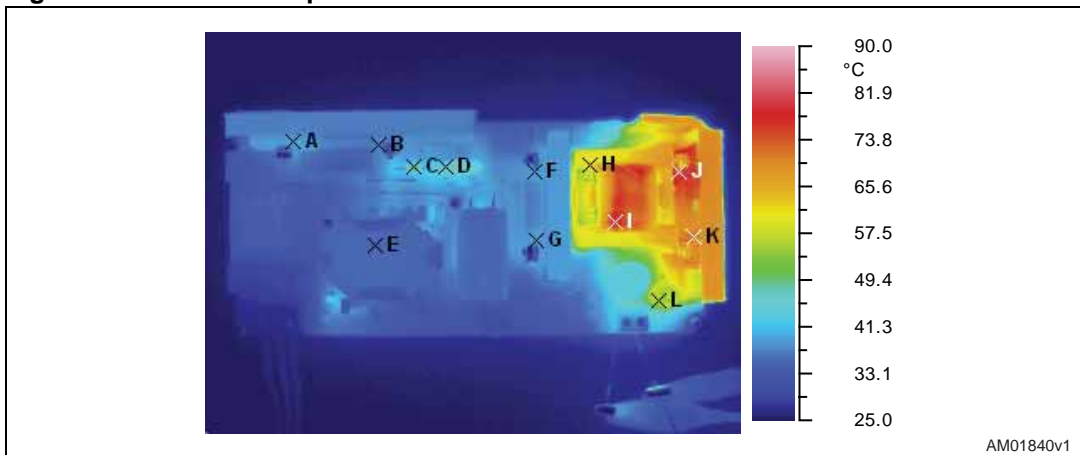


**Table 7. Temperature of key components ( $T_{amb} = 25\text{ }^{\circ}\text{C}$ , emissivity = 0.95 for all points)**

Point	Reference	T [ $^{\circ}\text{C}$ ] at 115Vac	T [ $^{\circ}\text{C}$ ] at 230Vac
A	D1 (Input bridge)	49.5	39.5
B	Q1 (PFC MOSFET)	46.4	37.9
C	D4 (PFC diode)	56.8	49.1
D	R6 (NTC)	55.9	47.1
E	L2 (PFC coil)	38.1	35.7
F	Q4 (AHB low-side MOSFET)	43.8	39.2

**Table 7. Temperature of key components ( $T_{amb} = 25\text{ °C}$ , emissivity = 0.95 for all points) (continued)**

Point	Reference	T [°C] at 115Vac	T [°C] at 230Vac
G	Q3 (AHB high side MOSFET)	40.2	39.3
H	T1 (AHB transformer ferrite)	64.8	63.4
I	T1 (AHB transformer winding)	81.2	80.1
J	D13 (AHB output diode)	83.1	81.8
K	D12 (AHB output diode)	73.7	72.8
L	L3 (Output inductor)	58.7	57.9

## 5 Conducted noise measurements (pre-compliance test)

Figure 26 and 27 show the conducted noise measurements performed at the two nominal voltages with peak detection and considering only the worst phase. Both measures are well below the average limit (taken from EN55022 CLASS B norm).

Figure 26. CE peak measure at 115Vac and full load

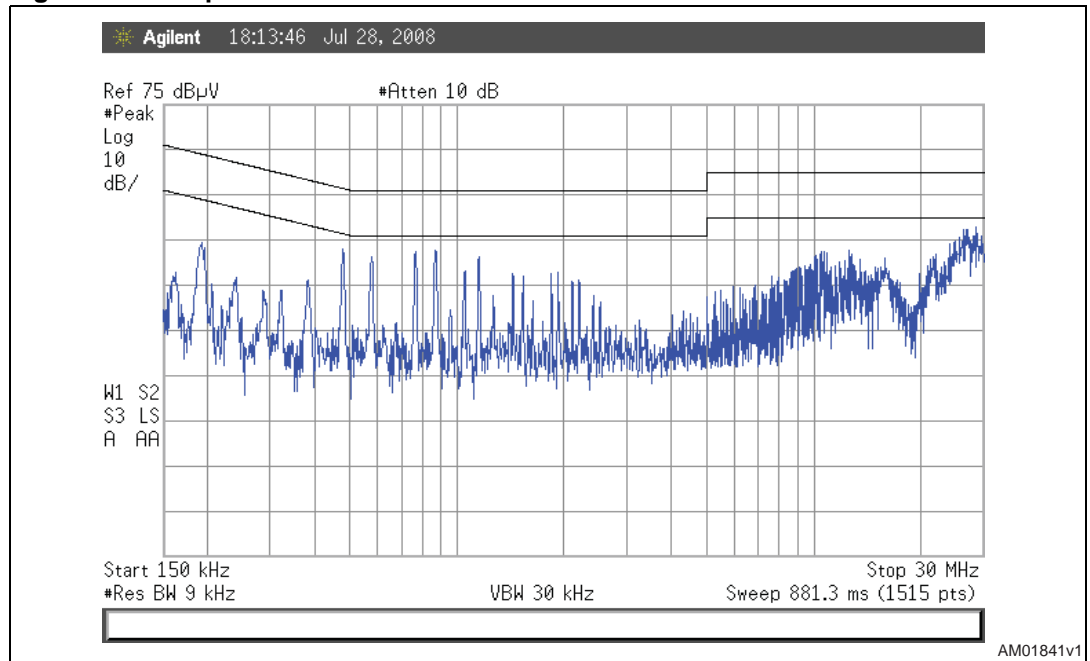
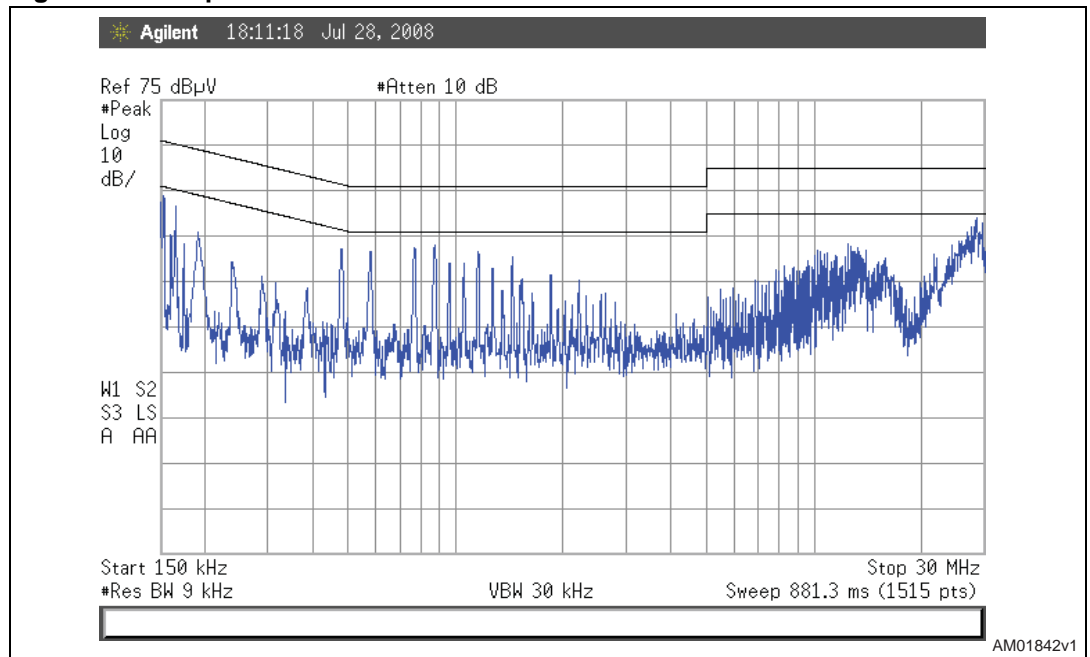


Figure 27. CE peak measure at 230Vac and full load





## 6 Bill of material

**Table 8. EVL6591-90WADP bill of materials**

Ref	Value	Description	Manufacturer
C1	470 NF	Polypropylene X2 capacitor - R46 KI 3470--02 M	Arcotronics
C10	1N0	SMD ceramic capacitor X7R - 50 V	AVX
C11	10 NF	SMD ceramic capacitor X7R - 50 V	AVX
C12	470 NF	SMD ceramic capacitor X7R - 25 V	AVX
C13	1 $\mu$ F	SMD ceramic capacitor X7R - 25 V	AVX
C14	100 NF	SMD ceramic capacitor X7R - 50 V	AVX
C15	22 $\mu$ F	Electrolytic capacitor YXF - 50 V	Rubycon
C16	1N0	SMD ceramic capacitor X7R - 50 V	AVX
C17	N.M.	Electrolytic capacitor	
C2	2N2	Ceramic Y1 capacitor - DE1E3KX222M	Murata
C20	2N2	Ceramic Y1 capacitor - DE1E3KX222M	Murata
C21	2N2	Ceramic Y1 capacitor - DE1E3KX222M	Murata
C22	220 PF	SMD ceramic capacitor NP0 - 50 V	AVX
C3	2N2	Ceramic Y1 capacitor - DE1E3KX222M	Murata
C39	100 NF	SMD ceramic capacitor X7R - 50 V	AVX
C4	470 NF	Polypropylene X2 capacitor - R46 KI 3470--02 M	Arcotronics
C40	10 NF	Ceramic capacitor X7R - 50 V	AVX
C41	4N7	SMD ceramic capacitor X7R - 50 V	AVX
C42	100 NF	SMD ceramic capacitor X7R - 50 V	AVX
C43	10 NF	SMD ceramic capacitor X7R - 50 V	AVX
C44	220 NF	Polypropylene capacitor - B32652A3224J	EPCOS
C45	220 PF	SMD ceramic capacitor NP0 - 50 V	AVX
C46	1000 $\mu$ F	Electrolytic capacitor ZL - 25 V	Rubycon
C47	2.2 NF	SMD ceramic capacitor X7R - 50 V	AVX
C48	6.8 NF	SMD ceramic capacitor X7R - 50 V	AVX
C49	330 PF	SMD ceramic capacitor NP0 - 50 V - 2%	AVX
C5	470 NF	Polypropylene capacitor - PHE426KD6470JR06L2	EVOX-RIFA
C50	100 NF	SMD ceramic capacitor X7R - 50 V	AVX
C51	22 $\mu$ F	Electrolytic capacitor YXF - 50 V	Rubycon
C52	100 NF	SMD ceramic capacitor X7R - 50 V	AVX
C53	N.M.	SMD ceramic capacitor X7R - 50 V	
C54	1 $\mu$ F	SMD ceramic capacitor X7R - 25 V	AVX

Table 8. EVL6591-90WADP bill of materials (continued)

Ref	Value	Description	Manufacturer
C55	N.M.	SMD ceramic capacitor X7R - 50 V	
C56	100 NF	SMD ceramic capacitor X7R - 50 V	AVX
C57	100 $\mu$ F	Electrolytic capacitor YXF - 35 V	Rubycon
C58	1N8	SMD ceramic capacitor X7R - 50 V	AVX
C59	470 PF	SMD ceramic capacitor X7R - 50 V	AVX
C61	N.M.	Electrolytic capacitor	
C62	N.M.	Electrolytic capacitor	
C9	47 $\mu$ F	Electrolytic capacitor - 450 V - EEUED2W470	Panasonic
D1	GBU6J	Bridge rectifier	Vishay
D12	STPS16L40CT	Power Schottky rectifier	STMicroelectronics
D13	STPS30100ST	Power Schottky rectifier	STMicroelectronics
D20	N.M.	Zener diode	
D21	1N4148	Diode	
D22	LL4148	SMD diode	
D23	LL4148	SMD diode	
D24	LL4148	SMD diode	
D25	BZV55-B13	Zener diode - 2%	Vishay
D26	STPS1L60A	SMD Schottky diode	STMicroelectronics
D27	LL4148	SMD diode	
D28	BZV55-B11	Zener diode - 2%	Vishay
D29	LL4148	SMD diode	
D3	1N4005	Diode	Vishay
D4	STTH2L06	Ultrafast diode	STMicroelectronics
F1	T4 A	PCB fuse TR5	Wickmann
J1	IN connector	Screw connector - MKDS 1,5/3-5.08	Phoenix Contact
J2	OUT connector	Screw connector - MKDS 1,5/2-5.08	Phoenix Contact
JP9	N.M.	Wire jumper	
L1	2x25 mH	Input EMI filter - HF2826-253Y1R2-T01	TDK
L2	700 $\mu$ H	PFC inductor - 1825.0001	Magnetica
L3	3.3 $\mu$ H	Power inductor - PCV-0-332-10L	Coilcraft
Q1	STP12NM50FP	Power MOSFET	STMicroelectronics
Q10	BC847C	Small signal BJT	
Q11	BC847C	Small signal BJT	
Q3	STP12NM50FP	Power MOSFET	STMicroelectronics
Q4	STP12NM50FP	Power MOSFET	STMicroelectronics

Table 8. EVL6591-90WADP bill of materials (continued)

Ref	Value	Description	Manufacturer
Q9	N.M.	Small signal BJT	
R1	1M0	SMD film resistor - 5% - 250 ppm/°C - 1206	Vishay
R10	15 kΩ	SMD film resistor - 1% - 100 ppm/°C - 0805	Vishay
R100	0R0	SMD film resistor - 1206	Vishay
R101	0R0	SMD film resistor - 1206	Vishay
R11	3M0	Film resistor - 1% - 100 ppm/°C - 0.4W	Vishay
R12	3M0	Film resistor - 1% - 100 ppm/°C - 0.4W	Vishay
R13	8.2 kΩ	SMD film resistor - 1% - 100 ppm/°C - 0805	Vishay
R14	18 kΩ	SMD film resistor - 5% - 250 ppm/°C - 1206	Vishay
R15	150 kΩ	SMD film resistor - 5% - 250 ppm/°C - 1206	Vishay
R17	0R0	SMD film resistor - 1206	Vishay
R18	56 kΩ	SMD film resistor - 5% - 250 ppm/°C - 0805	Vishay
R19	56 kΩ	SMD film resistor - 5% - 250 ppm/°C - 0805	Vishay
R2	1M2	SMD film resistor - 5% - 250 ppm/°C - 1206	Vishay
R20	0R0	SMD film resistor - 1206	Vishay
R21	27 Ω	SMD film resistor - 5% - 250 ppm/°C - 1206	Vishay
R22	0R47	Film resistor – 5% – 250 ppm/°C - 0.4W	Vishay
R23	0R47	Film resistor – 5% – 250 ppm/°C - 0.4W	Vishay
R24	1.8 kΩ	SMD film resistor - 1% - 100 ppm/°C - 0805	Vishay
R25	4.7 kΩ	SMD film resistor - 1% - 100 ppm/°C - 0805	Vishay
R26	240 kΩ	SMD film resistor - 5% - 250 ppm/°C - 0805	Vishay
R27	470	SMD film resistor - 5% - 250 ppm/°C - 1206	Vishay
R28	24K9	SMD film resistor - 1% - 100 ppm/°C - 0805	Vishay
R29	100 kΩ	SMD film resistor - 5% - 250 ppm/°C - 0805	Vishay
R3	680 kΩ	Film resistor - 1% - 100 ppm/°C - 1206	Vishay
R30	2K2	SMD film resistor - 1% - 100 ppm/°C - 1206	Vishay
R46	100 kΩ	SMD film resistor - 5% - 250 ppm/°C - 0805	Vishay
R53	0R0	SMD film resistor - 1206	Vishay
R54	0R0	SMD film resistor - 1206	Vishay
R55	0R0	SMD film resistor - 1206	Vishay
R6	2R5	NTC resistor S237 - B57237S0259M000	EPCOS
R69	N.M.	SMD resistor - 0805	Vishay
R7	680 kΩ	Film resistor - 1% - 100 ppm/°C - 0.4 W	Vishay
R70	33 Ω	SMD film resistor - 5% - 250 ppm/°C - 1206	Vishay
R71	10 Ω	SMD film resistor - 5% - 250 ppm/°C - 1206	Vishay

Table 8. EVL6591-90WADP bill of materials (continued)

Ref	Value	Description	Manufacturer
R72	10 $\Omega$	SMD film resistor - 5% - 250 ppm/ $^{\circ}$ C - 0805	Vishay
R73	100 k $\Omega$	SMD film resistor - 5% - 250 ppm/ $^{\circ}$ C - 0805	Vishay
R74	10 $\Omega$	SMD film resistor - 5% - 250 ppm/ $^{\circ}$ C - 0805	Vishay
R75	56 $\Omega$	SMD film resistor - 5% - 250 ppm/ $^{\circ}$ C - 0805	Vishay
R77	56 $\Omega$	SMD film resistor - 5% - 250 ppm/ $^{\circ}$ C - 0805	Vishay
R78	19K6	SMD film resistor - 1% - 100 ppm/ $^{\circ}$ C - 0805	Vishay
R79	100 k $\Omega$	SMD film resistor - 5% - 250 ppm/ $^{\circ}$ C - 0805	Vishay
R8	680 k $\Omega$	Film resistor - 1% - 100 ppm/ $^{\circ}$ C - 0.4 W	Vishay
R80	1K0	SMD film resistor - 5% - 250 ppm/ $^{\circ}$ C - 0805	Vishay
R81	0R82	SMD film resistor - 5% - 250 ppm/ $^{\circ}$ C - 1206	Vishay
R82	0R82	SMD film resistor - 5% - 250 ppm/ $^{\circ}$ C - 1206	Vishay
R83	6K8	SMD film resistor - 5% - 250 ppm/ $^{\circ}$ C - 0805	Vishay
R84	220 $\Omega$	SMD film resistor - 5% - 250 ppm/ $^{\circ}$ C - 1206	Vishay
R85	220 k $\Omega$	SMD film resistor - 1% - 100 ppm/ $^{\circ}$ C - 0805	Vishay
R86	33 k $\Omega$	SMD film resistor - 1% - 100 ppm/ $^{\circ}$ C - 0805	Vishay
R87	N.M.	SMD resistor - 0805	Vishay
R88	2K2	SMD film resistor - 5% - 250 ppm/ $^{\circ}$ C - 0805	Vishay
R89	100 k $\Omega$	SMD film resistor - 5% - 250 ppm/ $^{\circ}$ C - 1206	Vishay
R9	82 k $\Omega$	SMD film resistor - 1% - 100 ppm/ $^{\circ}$ C - 0805	Vishay
R90	0R0	SMD film resistor - 0805	Vishay
R91	75 k $\Omega$	SMD film resistor - 5% - 250 ppm/ $^{\circ}$ C - 0805	Vishay
R93	3K3	SMD film resistor - 1% - 100 ppm/ $^{\circ}$ C - 0805	Vishay
R94	12 $\Omega$	SMD film resistor - 5% - 250 ppm/ $^{\circ}$ C - 1206	Vishay
R95	47 $\Omega$	SMD film resistor - 5% - 250 ppm/ $^{\circ}$ C - 1206	Vishay
R96	470	SMD film resistor - 1% - 100 ppm/ $^{\circ}$ C - 1206	Vishay
R97	N.M.	SMD resistor - 1206	Vishay
R98	220 $\Omega$	SMD film resistor - 5% - 250 ppm/ $^{\circ}$ C - 1206	Vishay
R99	15 k $\Omega$	SMD film resistor - 5% - 250 ppm/ $^{\circ}$ C - 1206	Vishay
T1	Transformer	AHB transformer 1754.0004	Magnetica
U1	L6563	Advanced TM PFC controller	STMicroelectronics
U2	L6591	PWM controller for ZVS half-bridge	STMicroelectronics
U3	PC817	Optocoupler - PC817X1J000F	Sharp
U4	TS3431AILT	SMD voltage reference - 1%	STMicroelectronics
U5	PC817	Optocoupler - PC817X1J000F	Sharp

## 7 PFC coil specifications

- Application type: consumer, IT
- Transformer type: open
- Coil former: vertical type, 6+6 pins
- Max. temp. rise: 45°C
- Max. operating ambient temp.: 60°C
- Mains insulation: N.A.

### 7.1 Electrical characteristics

- Converter topology: boost, transition mode
- Core type: RM14 - N87 or equivalent
- Min. operating frequency: 20 kHz
- Primary inductance: 700  $\mu$ H 10% at 1 kHz - 0.25 V (see [Note 1](#))
- Peak primary current: 3.5 A<sub>pk</sub>
- RMS primary current: 1.25 A<sub>RMS</sub>

Note: 1 measured between pins 3-5

Figure 28. Electrical diagram

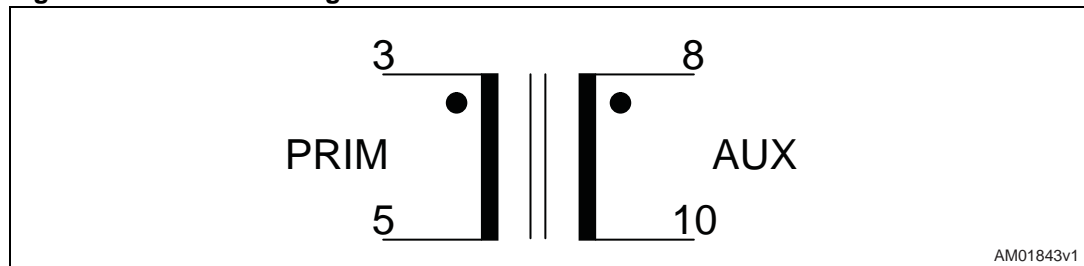


Table 9. Winding characteristics

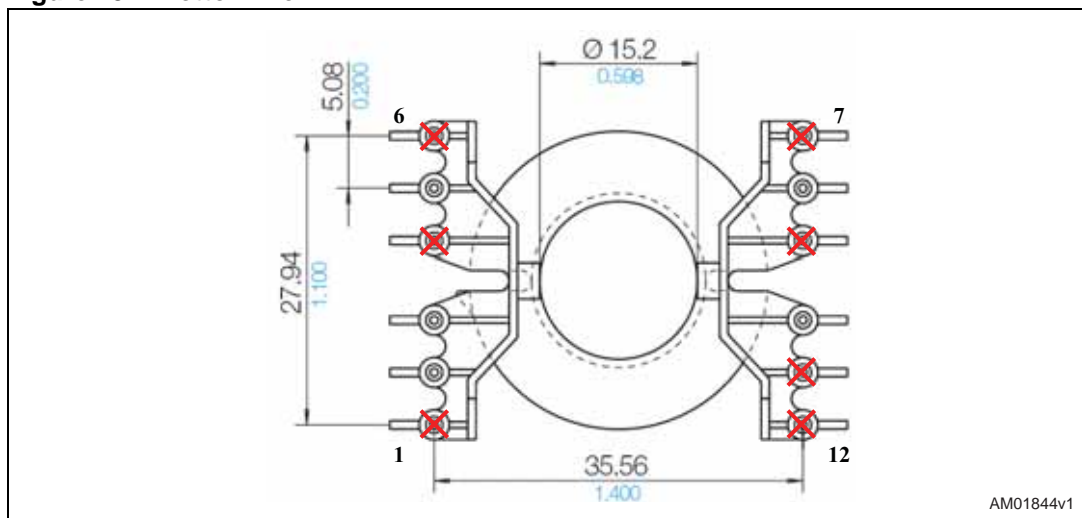
Pins	Winding	RMS current	Nr. of turns	Wire type
3 – 5	Primary	1.25 A <sub>RMS</sub>	53	Stranded 7 x Ø 0.28 mm – G2
8 – 10	AUX <sup>(1)</sup>	0.05 A <sub>RMS</sub>	4 spaced	Ø 0.28 mm – G2

1. Auxiliary winding is wound on top of primary winding

## 7.2 Mechanical aspect and pin numbering

- Maximum height from PCB: 22 mm
- Coil former type: vertical, 6+6 pins
- Pin distance: 5.08 mm
- Row distance: 35.56 mm
- Pins removed: # 1, 4, 6, 7, 9, 11, 12
- External copper shield: bare, wound around the ferrite core including the windings and coil former. Height is 7 mm. Connected by a solid wire soldered to pin 10
- Manufacturer: Magnetica
- P/N: 1825.0001.

Figure 29. Bottom view



## 8 AHB transformer specifications

- Application type: consumer, IT
- Transformer type: open
- Coil former: horizontal type, 7+7 pins
- Max. temp. rise: 45°C
- Max. operating ambient temp.: 60°C
- Mains insulation: compliance with EN60950.

### 8.1 Electrical characteristics

- Converter topology: asymmetrical half-bridge
- Core type: ETD34 - N87 or equivalent
- Operating frequency: 100 kHz
- Primary inductance: 400  $\mu\text{H}$  10% at 1 kHz - 0.25 V (see [Note 1](#))
- Air gap: 2.32 mm on central leg
- Leakage inductance: 10  $\mu\text{H}$  max. at 100 kHz - 0.25 V (see [Note 2](#))
- Primary capacitance: 6 pF typ. (see [Note 3](#))
- Max. peak primary current: 1.93  $A_{\text{pk}}$
- RMS primary current: 0.75  $A_{\text{RMS}}$

Note: 1 measured between pins 2-4

2 measured between pins 2-4 with secondaries and auxiliary windings shorted

3 calculated considering primary inductance and resonance frequency

Figure 30. Electrical diagram

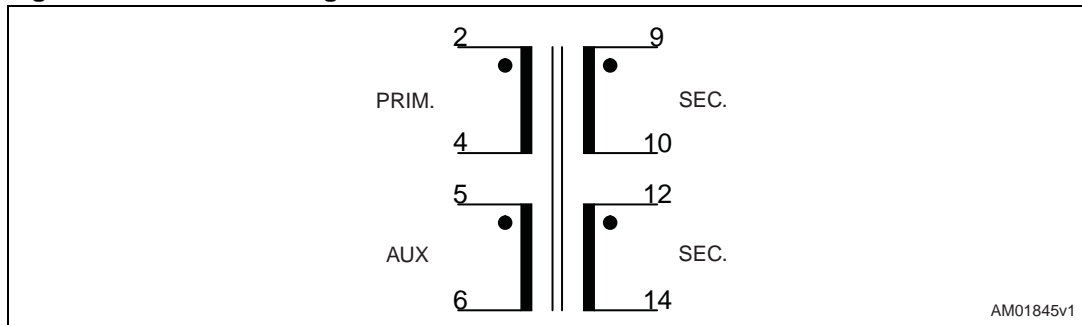
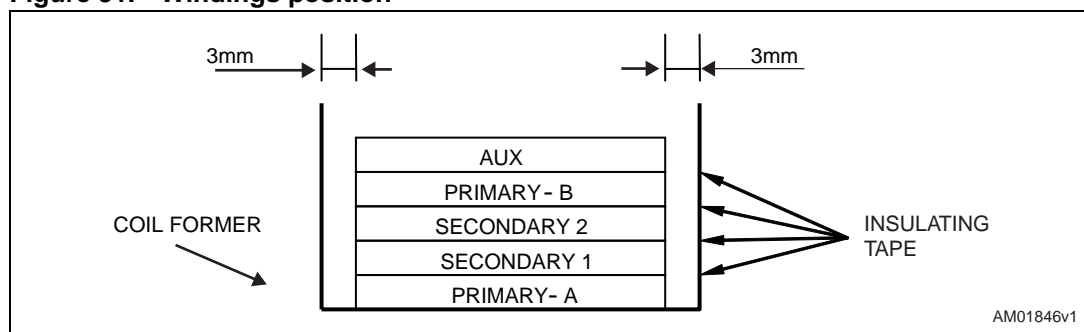


**Table 10. Winding characteristics**

Pins	Winding	RMS current	Nr. of turns	Wire type
2 – 3	Primary A	0.75 A <sub>RMS</sub>	35	Ø 0.355 mm – G2
9 – 10	Secondary 1	3.81 A <sub>RMS</sub>	4	Stranded 90 x Ø 0.1 mm – G1
12 – 14	Secondary 2	6.57 A <sub>RMS</sub>	7	Stranded 135 x Ø 0.1 mm – G1
3 – 4	Primary B	0.75 A <sub>RMS</sub>	35	Ø 0.355 mm – G2
5 – 6	Auxiliary	0.05 A <sub>RMS</sub>	3 spaced	Ø 0.355 mm – G2

Note: Primaries A and B are in series  
Cover wires ends with silicon sleeve

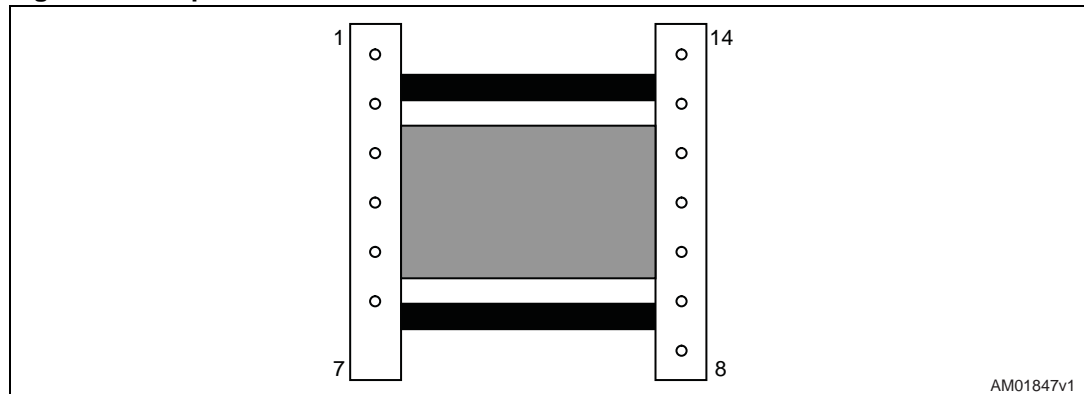
**Figure 31. Windings position**



## 8.2 Mechanical aspect and pin numbering

- Maximum height from PCB: 30 mm
- Coil former type: vertical, low profile, 7+7 pins, NORWE ETD34lr/h14/-1/rtg
- Pin distance: 5.08 mm
- Row distance: 25.4 mm
- Pin removed: # 7
- Manufacturer: Magnetica
- P/N: 1754.0004

**Figure 32. Top view**





# 9 PCB layout

Figure 33. Topside silk screen

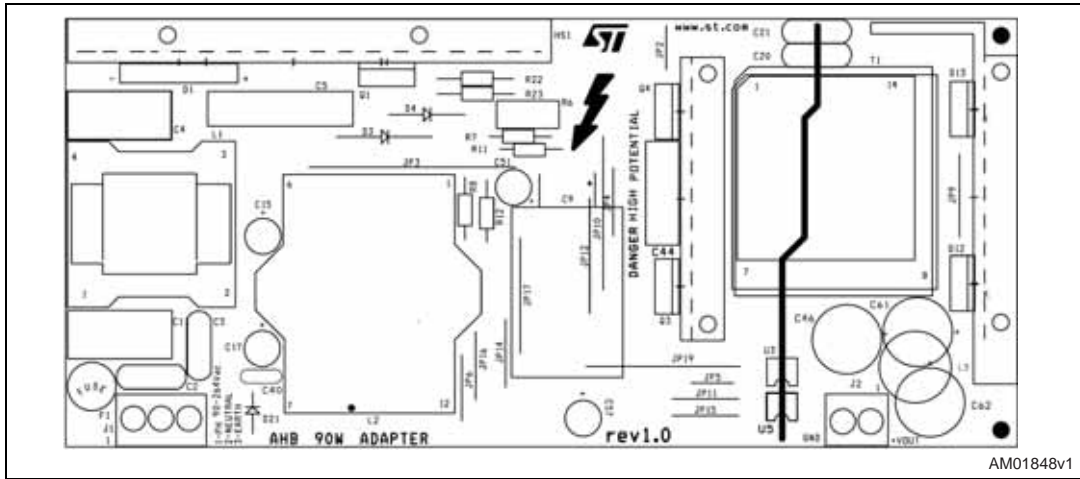


Figure 34. Bottomside silk screen

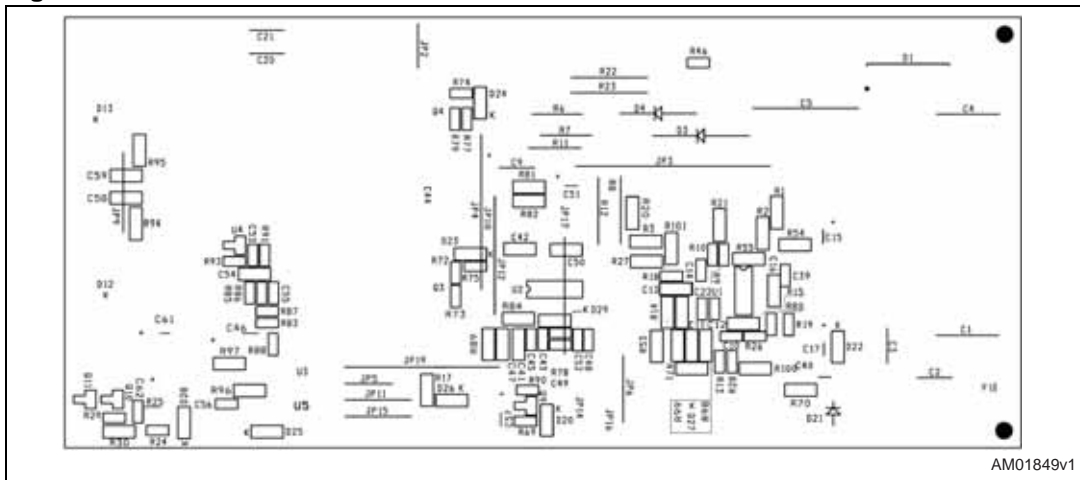
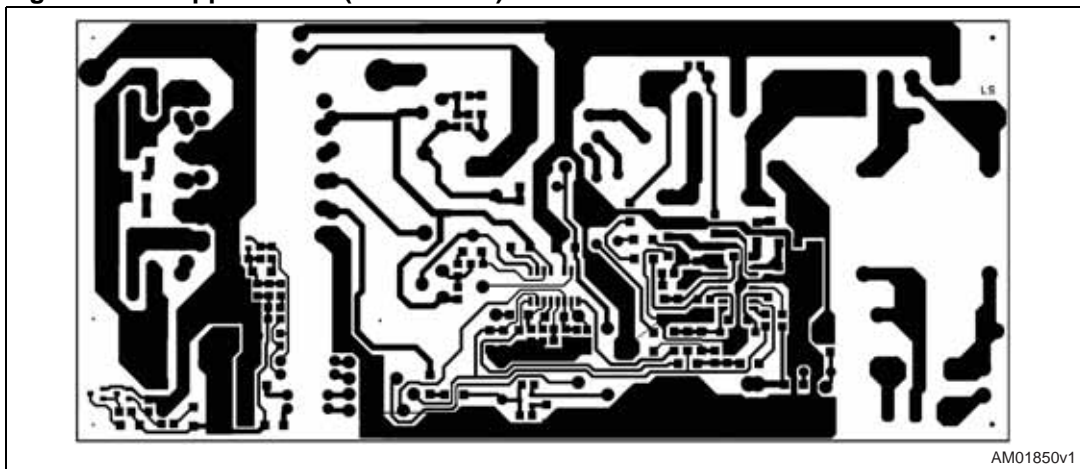


Figure 35. Copper traces (bottomside)



## 10 Revision history

**Table 11. Document revision history**

Date	Revision	Changes
28-Jan-2009	1	Initial release

**Please Read Carefully:**

Information in this document is provided solely in connection with ST products. STMicroelectronics NV and its subsidiaries ("ST") reserve the right to make changes, corrections, modifications or improvements, to this document, and the products and services described herein at any time, without notice.

All ST products are sold pursuant to ST's terms and conditions of sale.

Purchasers are solely responsible for the choice, selection and use of the ST products and services described herein, and ST assumes no liability whatsoever relating to the choice, selection or use of the ST products and services described herein.

No license, express or implied, by estoppel or otherwise, to any intellectual property rights is granted under this document. If any part of this document refers to any third party products or services it shall not be deemed a license grant by ST for the use of such third party products or services, or any intellectual property contained therein or considered as a warranty covering the use in any manner whatsoever of such third party products or services or any intellectual property contained therein.

**UNLESS OTHERWISE SET FORTH IN ST'S TERMS AND CONDITIONS OF SALE ST DISCLAIMS ANY EXPRESS OR IMPLIED WARRANTY WITH RESPECT TO THE USE AND/OR SALE OF ST PRODUCTS INCLUDING WITHOUT LIMITATION IMPLIED WARRANTIES OF MERCHANTABILITY, FITNESS FOR A PARTICULAR PURPOSE (AND THEIR EQUIVALENTS UNDER THE LAWS OF ANY JURISDICTION), OR INFRINGEMENT OF ANY PATENT, COPYRIGHT OR OTHER INTELLECTUAL PROPERTY RIGHT.**

**UNLESS EXPRESSLY APPROVED IN WRITING BY AN AUTHORIZED ST REPRESENTATIVE, ST PRODUCTS ARE NOT RECOMMENDED, AUTHORIZED OR WARRANTED FOR USE IN MILITARY, AIR CRAFT, SPACE, LIFE SAVING, OR LIFE SUSTAINING APPLICATIONS, NOR IN PRODUCTS OR SYSTEMS WHERE FAILURE OR MALFUNCTION MAY RESULT IN PERSONAL INJURY, DEATH, OR SEVERE PROPERTY OR ENVIRONMENTAL DAMAGE. ST PRODUCTS WHICH ARE NOT SPECIFIED AS "AUTOMOTIVE GRADE" MAY ONLY BE USED IN AUTOMOTIVE APPLICATIONS AT USER'S OWN RISK.**

Resale of ST products with provisions different from the statements and/or technical features set forth in this document shall immediately void any warranty granted by ST for the ST product or service described herein and shall not create or extend in any manner whatsoever, any liability of ST.

ST and the ST logo are trademarks or registered trademarks of ST in various countries.

Information in this document supersedes and replaces all information previously supplied.

The ST logo is a registered trademark of STMicroelectronics. All other names are the property of their respective owners.

© 2009 STMicroelectronics - All rights reserved

STMicroelectronics group of companies

Australia - Belgium - Brazil - Canada - China - Czech Republic - Finland - France - Germany - Hong Kong - India - Israel - Italy - Japan - Malaysia - Malta - Morocco - Singapore - Spain - Sweden - Switzerland - United Kingdom - United States of America

[www.st.com](http://www.st.com)

# Mouser Electronics

Authorized Distributor

Click to View Pricing, Inventory, Delivery & Lifecycle Information:

[STMicroelectronics:](#)

[EVL6591-90WADP](#)